Boehmite Dissolution Studies Supporting High Level Waste Pretreatment – 9383

R.A. Peterson, R.L. Russell, L.A. Snow
Pacific Northwest National Laboratory
P.O. Box 999, Richland, WA 99352

ABSTRACT

Boehmite is present in significant quantities in several of the Hanford waste tanks. It has been proposed that the boehmite will be dissolved through caustic leaching in the Hanford Waste Treatment and Immobilization Plant (WTP) currently under construction. Therefore, it is important to fully understand the nature of this dissolution so that the process can be effectively deployed.

This research determined the impact of primary control parameters on the boehmite dissolution rate. The impact of aluminate ion on the dissolution kinetics was determined. In addition, other parameters that impact boehmite dissolution, such as free-hydroxide concentration and reaction temperature, were also assessed and used to develop a semi-empirical model of the boehmite dissolution process. The understanding derived from this work will be used as the basis to evaluate and improve the planned performance of the WTP.

This work is the first in a series of programs aimed at demonstrating the WTP dissolution process. This work was used to develop a simulant of the boehmite-containing Hanford waste. That simulant is subsequently being used in laboratory- and pilot-scale testing to demonstrate the WTP pretreatment process in an integrated fashion.

INTRODUCTION

During the historical production of Pu at the Hanford Site from 1944 to the early 1970s, a significant volume of high level waste (HLW) sludge was produced and stored in tanks at the Hanford Site. The Waste Treatment and Immobilization Plant (WTP) under construction on the Hanford Site will be designed to separate the waste into two fractions for immobilization. After the HLW is separated from the low activity waste (LAW) liquid stream by ultrafiltration in the Pretreatment Facility (PTF), the concentrated HLW will undergo caustic and oxidative leaching processes to dissolve and wash out materials (aluminum, chromium, phosphates and sulfates) that would otherwise limit HLW loading in the glass waste form. The concentrated HLW solids will be sequentially caustic leached, washed, oxidatively leached, and washed once more during pretreatment. While the caustic leaching dissolves the aluminum in the HLW solids, the oxidative leaching is carried out to oxidize the chromium with a sodium permanganate ($NaMnO_4$) solution and dissolve it in a mild caustic solution. The HLW solids are concentrated after each leaching and washing operation using cross-flow ultrafiltration.

Caustic-leaching experiments were first performed on actual Hanford tank sludge samples in Fiscal Year (FY) 1993. The original caustic-leaching experiments were performed as a prelude to acid dissolution of the sludge solids with the intent that the acid-dissolved fraction would be processed through solvent extraction to separate the very small mass fraction of the radioactive elements (the transuranics [TRUs], ^{90}Sr and ^{137}Cs) from the bulk mass of non-radioactive components [1]. In this respect, caustic leaching was meant to remove the large amount of aluminum from the waste, thus reducing the nitric acid demand and simplifying the solvent extraction feed. Subsequently, however, caustic leaching was chosen as the baseline method for Hanford tank sludge pretreatment; this process was sometimes referred to as “Enhanced Sludge Washing” [2]. Following this decision, caustic-leaching tests were performed under a standard set of conditions at Pacific Northwest National Laboratory (PNNL) and Los Alamos National Laboratory; these tests were conducted from FY 1995 through FY 1997. In subsequent years, a limited

number of parametric caustic-leaching experiments were performed at PNNL and also at Oak Ridge National Laboratory. After establishing the Hanford WTP project, a limited number of laboratory-scale caustic-leaching experiments were performed using a standard testing protocol, but these were generally focused on processing double-shell tank wastes rather than the single-shell tanks where the bulk of the sludge is stored.

Caustic leaching data are needed on the various types of wastes to be processed through the WTP to support the plant design. The data needed include 1) removal of key HLW sludge components (e.g., Al, Cr, P, and S) as a function of caustic concentration, temperature, and time, 2) the behavior of radionuclides during the leaching process, 3) particle-size distribution before and after leaching, and 4) identification of the chemical and mineral forms of important sludge components (e.g., Al, Cr, and P) in the sludge solids. These data will be used to update the assessments of the expected performance of the WTP and to support the development of various waste simulants for scaled process demonstrations.

Aluminum in the wastes is believed to be present in the two most common mineralogical phases: gibbsite (monoclinic $Al(OH)_3$) and boehmite (orthorhombic AlOOH). Other Al-containing phases present include bayerite, dawsonite, alumina silicates, and amorphous aluminum hydroxide. The dissolution rates of the two primary mineralogical phases are considerably different. Therefore, the leaching kinetics will depend on the relative amounts of these phases in the waste as well as particle size, crystal habit (i.e., particle size and shape), operating temperature, hydroxide activity, aluminum solubility limits, particle Reynolds number associated with the mixing system, etc. The other aluminum compounds in the waste solids are present in relatively smaller amounts and therefore are considered less significant to the caustic leaching for removing aluminum from the HLW.

Recently, a series of characterization tests have been performed to support quantification of the various types of aluminum present in the Hanford HLW. Table I shows a breakdown of the Al sources in Hanford HLW. Values are shown in terms of the mass of aluminum associated with each phase. Inspection of the figure indicates that most of the aluminum is either sodium aluminate (supernate and water soluble) or gibbsite. The next major component is boehmite. The boehmite represents the largest component for which aggressive leaching conditions are required to achieve dissolution. As such, understanding the boehmite leaching chemistry and the impacts on the WTP flowsheet will be the focus of this article.

Table I. Sources of Al in Hanford Tank Waste.

Al Source	Metric Ton of Al
Supernate	1,188
Water Soluble	1,297
Easy to Dissolve	306
Gibbsite	3,022
Boehmite	1,775
Unassigned	568
Intractable	552
Total	8,708

EXPERIMENTAL

This section describes the methods used to conduct the leach testing for both actual waste samples and simulant samples.

Actual Waste Testing

Details of the experimental methods used during leaching experiments with actual high-boehmite tank waste can be found in Fiskum et al. [3]. The following is a synopsis of the testing performed. A portion of the sample slurry containing 17 g of water-insoluble solids was centrifuged (at ~960 G) for 20 minutes, and the supernatant was removed. The centrifuged solids were washed three times with 110 mL (3× the centrifuged solids volume) of 0.01 M NaOH. Each washing step consisted of mixing for 15 minutes using an overhead stirrer, centrifuging, and decanting the washing liquor.

After the initial washing step, deionized water was added to yield a slurry containing 17 g solids in 905 g of slurry (i.e., 1.9 wt% undissolved solids [UDS]). This provided a slurry with rheological properties suitable for subdividing the material. An overhead mixer equipped with a 3-bladed stainless steel impeller was used to homogenize the thinned slurry, and thirteen ~66.5 g slurry samples were transferred to 125-mL high-density polyethylene (HDPE) bottles with a large disposable polyethylene pipet. Each sample contained ~1.25 g UDS. One additional sample containing approximately 21.0 g of slurry (equivalent to 0.4 g dry solids) was transferred to a 60-mL HDPE bottle. The latter sample was analyzed by inductively couple plasma-optical emission spectrometry (ICP-OES), X-ray diffraction (XRD), and transmission electron microscopy (TEM) to establish the starting composition of the washed solids.

Table II summarizes the leaching conditions used for each of the 13 samples. Note that these conditions reflect the final supernate composition, but these compositions did not change substantively during the testing. The test matrix evaluated the effects of free-hydroxide concentration (1 to 5 M NaOH), temperature (80 to 100°C), and sodium nitrate concentration (1 to 5 M $NaNO_3$) on boehmite leaching kinetics.

Table II. Group 5 Caustic Leaching Conditions

Bottle ID	Free [OH], M		[Na], M		$[NO_3^-]$, M		Temperature, C[b]
	Target	Measured[a]	Target	Measured[a]	Target	Measured[a]	
G5-80-1	1	0.97	1	1.15	NA	NA	80[c]
G5-80-3	3	3.30	3	3.52	NA	NA	80[c]
G5-80-5	5	5.06	5	5.33	NA	NA	80[c]
G5-90-1	1	0.91	1	1.18	NA	NA	90
G5-90-3a	3	2.94	3	3.22	NA	NA	90
G5-90-3b	3	2.90	3	3.21	NA	NA	90
G5-90-3c	3	3.02	3	3.25	NA	NA	90
G5-90-1N-3	3	3.13	4	4.22	1	1.11	90
G5-90-5N-3	3	3.06	8	8.46	5	5.13	90
G5-90-5	5	5.01	5	5.16	NA	NA	90
G5-100-1	1	0.86	1	1.11	NA	NA	100
G5-100-3	3	2.81	3	3.22	NA	NA	100
G5-100-5	5	5.11	5	5.58	NA	NA	100

[a] The measured analyte concentrations represent the equilibrium concentration obtained after a 170-h contact time.
[b] The temperature uncertainty was ±2.5°C.
[c] Loss of temperature control occurred after 72 h process time.

The general procedure used for the leaching experiments with actual tank waste was as follows. Sodium hydroxide (19 M) and water were added to yield the desired NaOH concentration and a total slurry volume of 100 mL. In the case of leaching samples G5-90-1N-3 and G5-90-5N-3, solid $NaNO_3$ was added in sufficient quantity to meet the target nitrate concentration. Each leaching vessel was closed with

a cap equipped with a tube condenser to eliminate pressurization and minimize water loss. The sample slurries were placed in a temperature-controlled aluminum heating block installed on a shaker table. The shaking speed was digitally controlled to 200 rpm.

The leaching mixtures were shaken for 170 hours at the desired temperature. Samples were withdrawn at 1, 4, 8, 24, 72, and 170 hours to assess the aluminum dissolution kinetics. At the conclusion of the 170–hour leaching period, additional leachate samples were taken to determine the free-hydroxide ion concentration, gamma emitters by gamma energy analysis, and Cr(VI) by ultraviolet visible spectrophotometry. The equilibrium concentration values for free hydroxide, sodium, and nitrate are shown in Table II and were based on results from the samples taken at 170 hours.

Samples of the washed tank waste solids were examined by powder XRD. The specimens were pulverized to a powder with a boron carbide mortar and pestle, mixed with an internal standard (rutile, TiO_2, or alumina, Al_2O_3), and mounted on a glass slide. In some cases, the internal standard was omitted in an effort to provide better clarity of the sample diffraction pattern free from potential interference from the internal standard diffraction pattern. Process parameters included examination of the X-ray 2-theta range from 5 to 65 degrees with a step size of 0.02 degrees and a dwell time of 20 seconds. Phase identification was performed with JADE, Version 8.0 (Materials Data Inc., Livermore, CA) software search and peak match routines with comparison to the International Centre for Diffraction Data (ICDD) database PDF-2, Version 2.0602 (2006). The ICDD database included the Inorganic Crystal Structure Database (ICSD) maintained by Fachinformationszentrum, Karlsruhe, Germany. Phase identification incorporated chemistry restrictions based on the elements determined from chemical analysis.

Surface areas were measured according to American Society for Testing and Materials method D5604-96, Test Method B (Single-Point Surface Area by Flowing Gas Apparatus). The flow gas used in the measurement mode was composed of 30% nitrogen in helium. The system was calibrated per manufacturer instructions. The system performance was assessed using a 29.9 ± 0.75 m^2/g carbon surface area standard Lot D-6 obtained from Micromeritics (Norcross, GA). To prepare the samples for the surface-area measurement, the solids were rinsed twice with ethanol and twice again with ethyl ether. Each rinse was conducted in a centrifuge tube. The solids were well suspended in the rinse solution, and then the phases were separated by centrifuging and decanting. The final ethyl ether rinse was used to transfer the solids slurry to the sample cell. The ethyl ether was then evaporated at room temperature directly from the sample cell.

Simulant Testing

Simulant boehmite was obtained from APYRAL (for product information, see: http://www.nabaltec.de/download/produkte/Apyral_16-32_Datasheet_DE-EN.PDF), product AOH 20. XRD analysis confirmed that this material is boehmite. The simulant tests were performed in a 1-L reaction vessel. The vessel was filled with the leaching fluid and heated to 100°C. The temperature was measured with a calibrated thermocouple and controlled with a calibrated temperature controller. Boehmite was added as a powder to the reaction vessel through the sample port while stirring, which started the clock for the test. The test solution was sampled at 1, 2, 4, 8, and 24 hours. Each sample consisted of 5 mL supernatant, which was filtered after being drawn from the reaction vessel and then analyzed for aluminum and sodium.

RESULTS

Sample Characterization

For the washed tank waste solids, the XRD pattern and the chemical analysis were used to estimate the different compounds in the sample. The approximate mass percent of chemical phases was determined by evaluating the crystalline species in conjunction with the elemental concentrations. Nominally 90 wt% of the solids was identified; ~7% of the sodium content could not be tied to a specific phase. Table III summarizes the estimated mass percent of the various phases in the solids. Phases were listed as "observed" if recognized in the XRD pattern; phases were "assigned" based on chemical analysis and assumptions about the tank chemistry. The entrained-salts component was determined from the calculated dilution of entrained supernatant in the wet centrifuged solids. The three sequential washings at an ~1:1 liquid-to-solids phase ratio were not sufficient to remove all of the supernatant. As intended, this waste sample was clearly dominated by boehmite.

Table III. Weight Percent of Mineral Phases, Best Estimate

Crystalline Phase	**Chemical Structure**	**Weight %**	**Basis**
Boehmite	AlOOH	66.8	Observed
Gibbsite	$Al(OH)_3$	5.1	Observed
Zeolite A (prototypic)	$NaSiAlO_4$	3.1	Assigned
Sodium uranium oxide	$Na_2U_2O_7$	2.6	Observed
Cancrinite	$Na_6Ca_2Al_6Si_6O_{24}(CO_3)_2$	1.7	Assigned
Iron oxide	Fe_2O_3	1.0	Observed
Manganese dioxide	MnO_2	0.71	Assigned
Unaccounted sodium	Na (in Al matrix)	6.7	Assigned
Chromium hydroxide	$Cr(OH)_3$	0.42	Assigned
Nickel hydrogen phosphate hydrate	$Ni(H_2PO_2)_2(H_2O)_6$	0.16	Observed
Strontium oxide	SrO	0.14	Assigned
Entrained Na salts from supernatant	various	9.3	Observed
Sum		97.6	

The TEM micrographs of the solids phase are shown in Figure 1. The material had a relatively high surface area with small particles, was dominated by Al phases, and the specific particle morphology of Al phases was identified as boehmite (identified by its rhombohedral platelet-like morphology). Spherical and elongated particles also were evident that appeared to be associated with more dense material consistent with U, Mn, and Fe species.

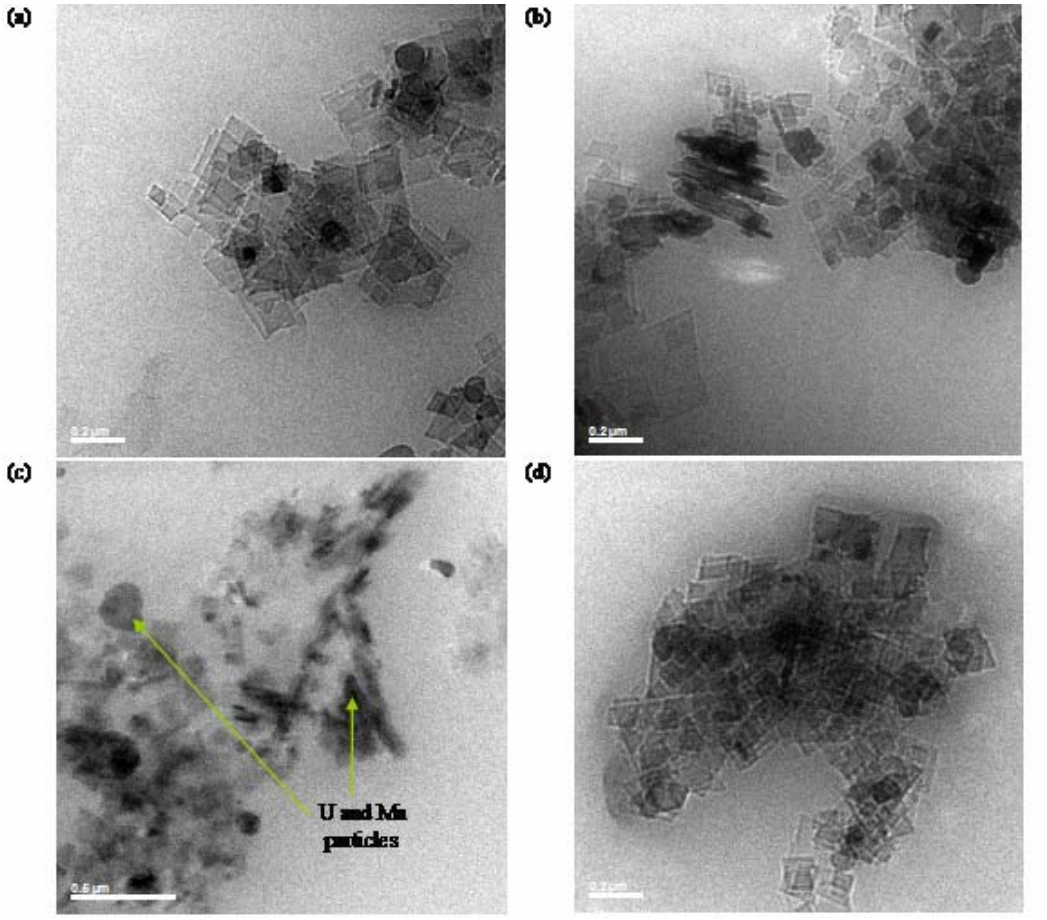

Fig. 1. TEM images of actual waste boehmite solids.

Boehmite is sometimes observed to be fibrous or acicular, so such observations are not always diagnostic. In the presence of nitrate, boehmite is known to precipitate as hexagonal plates [4]. The morphology of gibbsite crystals evolves from thin, rounded hexagons and faceted lozenges into faceted plates and blocks with well-formed basal prismatic faces. Caustic conditions, not just reaction time, are known to lead to the formation of larger crystals. Crystal dimensions ranged from 0.1 to 0.2 microns.

Figure 2 shows a scanning electron microscopy (SEM) micrograph of the commercially procured boehmite that was used in the simulant tests. Note that the average crystal size for this material is approximately 0.8 microns. The material agglomerates into larger particles, so particle-size distribution measurements do not provide significant insight into the reactivity of the boehmite.

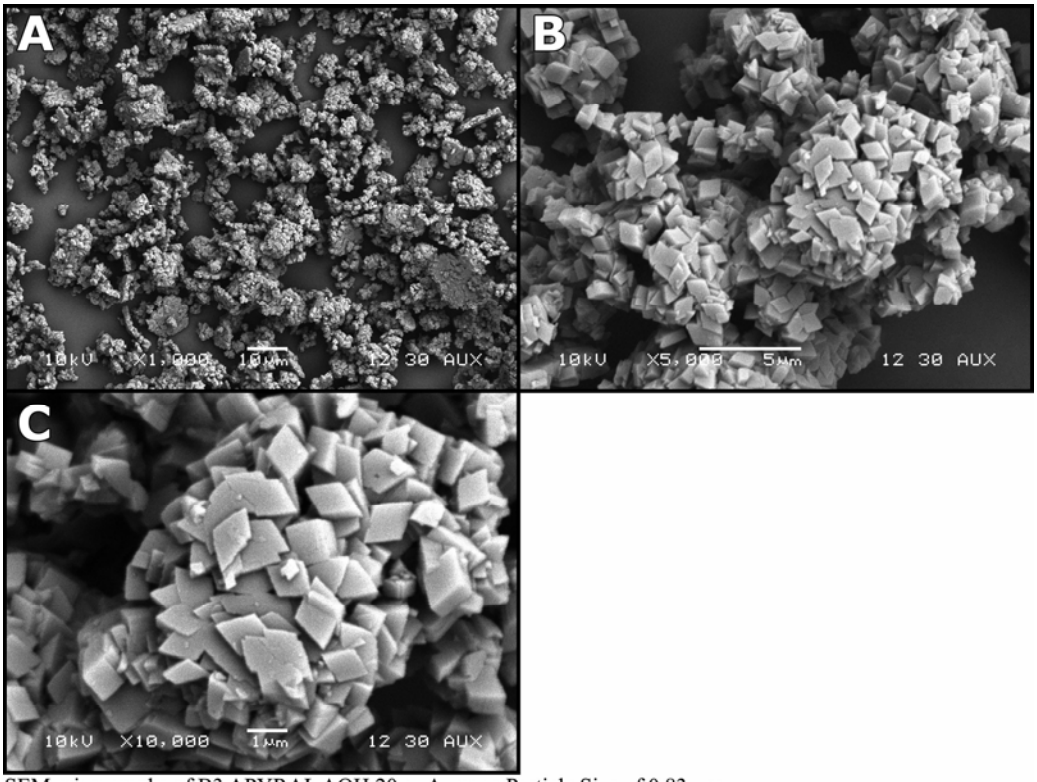

Fig. 2. SEM micrograph of simulant boehmite.

Table IV compares the surface area of the actual tank waste sample to that of the boehmite used in the simulant. As might be expected from the smaller primary particle size, the surface area of the actual tank waste material was significantly larger than for the commercially procured boehmite.

Table IV**.** Surface Area of Boehmite Samples

Sample ID	Specific Surface Area (m^2/g)
Washed Tank Waste Solids	26
Simulant Boehmite	10.22

Aluminum Dissolution Studies

The dissolution of boehmite is generally expressed as:

$$AlOOH + OH^- + H_2O \Leftrightarrow Al(OH)_4^- \quad \text{(Eq. 1)}$$

At a given condition, this can be written as

$$\frac{dAlOOH}{dt} = -k_f (OH)^- + k_r Al(OH)_4^- \quad \text{(Eq. 2)}$$

Where kf includes a surface area term associaeted with the boehmite surface. At saturation, this can be written as

$$\frac{dAlOOH}{dt} = 0 \therefore k_f (OH)_s^- = k_r Al(OH)_{4,s}^- \quad \text{(Eq. 3)}$$

Substituting produces:

$$\frac{dAlOOH}{dt} = -k_f (OH)^- + k_f \frac{(OH)_s^-}{Al(OH)_{4,s}^-} Al(OH)_4^- \quad \text{(Eq. 4)}$$

If we assume a relatively large excess of hydroxide:

$$\frac{dAlOOH}{dt} = -k_f (OH)^- \left(1 - \frac{Al(OH)_4^-}{Al(OH)_{4,s}^-}\right) \quad \text{(Eq. 5)}$$

Or

$$\frac{dAlOOH}{dt} = -k_f (OH)^- (1-\sigma) \quad \text{(Eq. 6)}$$

where

$$\sigma = \frac{Al(OH)_4^-}{Al(OH)_{4,s}^-} \quad \text{(Eq. 7)}$$

Then, adding the surface area dependence

$$\frac{dAlOOH}{dt} = -kA_B (OH)^- (1-\sigma) \quad \text{(Eq. 8)}$$

where, based on a shrinking core model:

$$A_B \propto AlOOH^{2/3} \quad \text{(Eq. 9)}$$

$$\frac{A_B}{A_{B.i}} = \left(\frac{AlOOH}{AlOOH_i}\right)^{2/3} \quad \text{(Eq. 10)}$$

$$\frac{d\left(\frac{AlOOH}{AlOOH_i}\right)}{dt} = -k\left(\frac{AlOOH}{AlOOH_i}\right)^{2/3} (OH)^- (1-\sigma) \quad \text{(Eq. 11)}$$

One series of comparisons between the simulant and actual waste results are shown in Table V. In these tests, the simulant conditions were effectively identical to those of the actual waste tests. The initial matrix consisted solely of sodium hydroxide, and the dissolution of boehmite was tracked as a function of time. Here, one can see that there was reasonable agreement between the dissolution rates for the procured boehmite and for the actual waste boehmite in both 3 M and 5 M NaOH.

Table V. Measured Fraction Boehmite Dissolved for Simulant and Actual Waste Samples

Reaction Time	Actual Waste 3 M NaOH	Actual Waste 5 M NaOH	Simulant 3 M NaOH	Simulant 5 M NaOH
0	-	-	0.00	0.00
1	0.09	0.13	0.10	0.12
2	-	-	0.17	0.22
4	0.32	0.44	0.28	0.37
8	0.51	0.65	0.49	0.60
24	0.82	0.91	0.94	0.99

However, a second set of simulant tests were run where the initial matrix contained varying amounts of sodium aluminate. In these tests, the initial supernate contained various levels of soluble aluminate before the start of leaching. Initial rate measurements from these tests are plotted in Figure 3 as a function of the initial aluminate concentration represented as a fraction of the boehmite solubility limit at 100°C. Inspection of Figure 3 indicates that while the initial reaction rate in the absence of aluminate is roughly the same for the simulant and actual waste (as indicated in Table IV), the reaction rate at higher aluminate levels drops significantly for the simulant. As indicated in Eq. 11, the dissolution rate is expected to decrease linearly with increasing approach to the solubility limit. After the initial drop in reaction rate for the simulant, the initial rate data appear to be following the linear trend expected for increasing initial aluminate concentration. These data were fit to a linear expression (the solid line in Figure 3). This fit was then adjusted to project the actual waste dissolution behavior based on the surface-area measurements shown in Table IV. Inspection of Figure 3 indicates that this projection agrees very well with the measured actual waste dissolution rate.

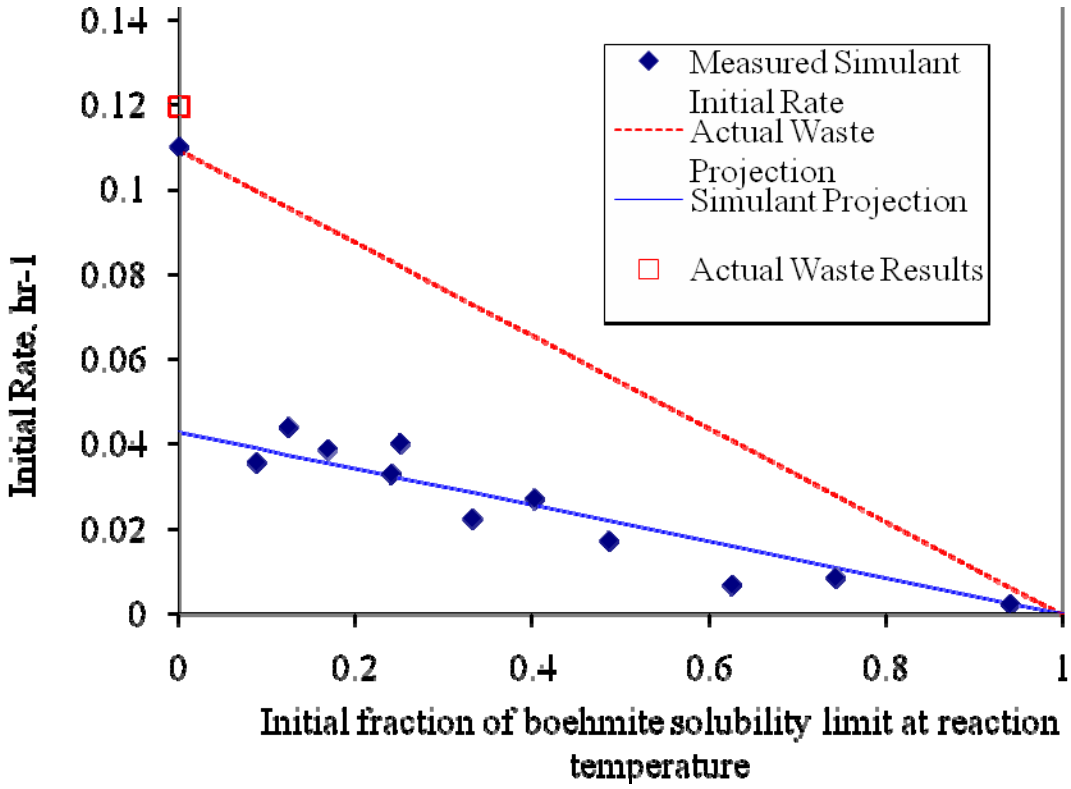

Fig. 3. Boehmite dissolution rate as a function of approach to the solubility limit.

These results suggest there may be two regimes that control the boehmite dissolution of simulant material. In the first regime, a fast reaction takes place in the absence of aluminate. This first reaction may be associated with a phenomena similar to the adsorption of a layer of aluminate on the surface of the boehmite crystals. Once this layer is developed—either through a reaction or through the presence of bulk aluminate—the reaction slows to one governed by the disassociation rate of the aluminate from the surface. Under this slower regime, the disassociation rate would be a direct function of the approach to the solubility limit as indicated in Figure 3. Further, the results suggest that the actual waste material is governed only by this second dissolution regime as indicated by the strong agreement between the reaction rate for the actual waste projected based on the surface area differences and the measured actual waste reaction rate as shown in Figure 3.

CONCLUSIONS

Based on the discussion above, it appears that the simulant used will react approximately 2.6 times slower than actual waste under most typical process conditions. However, once sufficient aluminate is present to suppress the initial fast rate for the simulant, the rate-limiting step for both the simulant and actual waste appear to be the same. As such, any scaled results obtained with the simulant can be expected to produce the same kinetically scaled results for the actual waste. A logical extension of this work would be to verify these assumptions by performing additional actual waste tests at higher initial aluminate concentrations.

REFERENCES

1. G.J. LUMETTA, B.M. RAPKO, M.J. WAGNER, J. LIU, and Y.L. CHEN, *Washing and Caustic Leaching of Hanford Tank Sludges: Results of FY 1996 Studies*, PNNL-11278, Pacific Northwest National Laboratory, Richland, Washington (1996).

2. G.J. LUMETTA, B.M. RAPKO, J. LIU, D.J. TEMER, and R.D. HUNT, *Washing and Caustic Leaching of Hanford Tank Sludge: Results of FY 1998 Studies*, PNNL-12026, Pacific Northwest National Laboratory, Richland, Washington (1998).

3. S.K. FISKUM, E.C. BUCK, R.C. DANIEL, K. DRAPER, M.K. EDWARDS, T.L. HUBLER, L.K. JAGODA, E.D. JENSON, G.J. LUMETTA, B.K. McNAMARA, R.A. PETERSON, S.I. SINKOV, and L.A. SNOW, *Characterization and Leach Testing for REDOX Sludge and S-Saltcake Actual Waste Sample Composites*, PNNL-17368 (WTP-RPT-157), Pacific Northwest National Laboratory, Richland, Washington (2008).

4. S. MUSIC, D. DRAGCEVIC, S. POPOVIC, and N. VDOVIC, “Microstructural Properties of Boehmite Formed Under Hydrothermal Conditions,” *Materials Science and Engineering B* 52(2-3):145-153 (1998).